Dissipative particle dynamics simulations of polymer-protected nanoparticle self-assembly

Cite as: J. Chem. Phys. **135**, 184903 (2011); https://doi.org/10.1063/1.3653379
Submitted: 27 June 2011 . Accepted: 27 September 2011 . Published Online: 09 November 2011

Justin R. Spaeth, Ioannis G. Kevrekidis, and Athanassios Z. Panagiotopoulos

Dissipative particle dynamics simulations of polymer-protected nanoparticle self-assembly

Justin R. Spaeth,[1,a)] Ioannis G. Kevrekidis,[1,2] and Athanassios Z. Panagiotopoulos[1,3]
[1]*Department of Chemical and Biological Engineering, Princeton University, Princeton, New Jersey 08544-5263, USA*
[2]*Program in Applied and Computational Mathematics, Princeton University, Princeton, New Jersey 08544-5263, USA*
[3]*Institute for the Science and Technology of Materials, Princeton University, Princeton, New Jersey 08544-5263, USA*

(Received 27 June 2011; accepted 27 September 2011; published online 9 November 2011)

Dissipative particle dynamics simulations were used to study the effects of mixing time, solute solubility, solute and diblock copolymer concentrations, and copolymer block length on the rapid co-precipitation of polymer-protected nanoparticles. The simulations were aimed at modeling Flash NanoPrecipitation, a process in which hydrophobic solutes and amphiphilic block copolymers are dissolved in a water-miscible organic solvent and then rapidly mixed with water to produce composite nanoparticles. A previously developed model by Spaeth *et al*. [J. Chem. Phys. **134**, 164902 (2011)] was used. The model was parameterized to reproduce equilibrium and transport properties of the solvent, hydrophobic solute, and diblock copolymer. Anti-solvent mixing was modeled using time-dependent solvent-solute and solvent-copolymer interactions. We find that particle size increases with mixing time, due to the difference in solute and polymer solubilities. Increasing the solubility of the solute leads to larger nanoparticles for unfavorable solute-polymer interactions and to smaller nanoparticles for favorable solute-polymer interactions. A decrease in overall solute and polymer concentration produces smaller nanoparticles, because the difference in the diffusion coefficients of a single polymer and of larger clusters becomes more important to their relative rates of collisions under more dilute conditions. An increase in the solute-polymer ratio produces larger nanoparticles, since a collection of large particles has less surface area than a collection of small particles with the same total volume. An increase in the hydrophilic block length of the polymer leads to smaller nanoparticles, due to an enhanced ability of each polymer to shield the nanoparticle core. For unfavorable solute-polymer interactions, the nanoparticle size increases with hydrophobic block length. However, for favorable solute-polymer interactions, nanoparticle size exhibits a local minimum with respect to the hydrophobic block length. Our results provide insights on ways in which experimentally controllable parameters of the Flash NanoPrecipitation process can be used to influence aggregate size and composition during self-assembly. © *2011 American Institute of Physics*. [doi:10.1063/1.3653379]

I. INTRODUCTION

Flash NanoPrecipitation is a technique developed by Johnson and Prud'homme[1–3] that uses rapid mixing of solvent and anti-solvent to produce kinetically "frozen" nanoparticles. The initial step of the technique involves dissolving a diblock copolymer and a hydrophobic solute (e.g. a drug molecule or imaging agent) in a suitable solvent, such as tetrahydrofuran (THF). The diblock copolymer contains a hydrophobic block and a hydrophilic block (usually polyethylene glycol, PEG). The THF solution is then rapidly mixed with water in a device with a characteristic mixing time on the order of a few milliseconds.[4,5] As the mixing progresses, the solvent quality becomes poorer and nanometer-sized solute clusters form, with the hydrophobic blocks of the polymers aggregating onto the clusters. The hydrophilic blocks extend out from the nanoparticles, providing steric stabilization against fusion. This technique has been used to produce nanoparticles of controllable size with different constituent polymers and solutes.[6–15] Potential applications of these materials include drug delivery and medical imaging.

Although Flash NanoPrecipitation has been successfully used to prepare nanoparticles, a detailed microscopic understanding of the process is still lacking. Experimentally, only the initial and final states of the system are observable, using direct imaging or scattering techniques. Observing the dynamics of the aggregation process is not feasible, since its characteristic time scales are ns to ms. In addition, the influence of experimentally controllable parameters such as the mixing time, solute and polymer concentrations, and block copolymer architecture on the self-assembly process has only been examined for a few cases. No systematic framework is available for understanding how these parameters influence the size and internal structure of the nanoparticles. In this work, we utilize a previously developed

a)Author to whom correspondence should be addressed. Electronic mail: jspaeth@princeton.edu.

dissipative particle dynamics (DPD) model to study these effects.

In a recent simulation study,[16] implicit- and explicit-solvent models of the Flash NanoPrecipitation process were developed. The experiments of Kumar *et al.*[15] served as a reference point for the parameterization of the model. In particular, in Ref. 15 Itraconazole, an antifungal drug, was the hydrophobic solute, polystyrene-*b*-polyethylene glycol (PS_{10}-*b*-PEG_{68}) was the diblock copolymer, and THF and water were the solvent and anti-solvent, respectively. The implicit-solvent (Brownian Dynamics) approach produced incorrect aggregation dynamics and incorrect scaling of aggregate diffusion coefficients with particle size. On the other hand, the explicit-solvent approach, based on dissipative particle dynamics simulations, produced reasonable aggregation dynamics and reproduced the correct Stokes-Einstein scaling of diffusion coefficients with particle size. The primary aim of this previous work was to compare and contrast the implicit and explicit solvent approaches. The simplifying assumption that mixing occurs instantaneously was made; all simulations were performed with the same solute and copolymer concentrations, and with the same copolymer architecture. No detailed parametric study of the effects of experimentally controllable parameters of Flash NanoPrecipitation on final particle size was performed in the prior study. The main objective of the current manuscript is to achieve a qualitative understanding of these effects, by investigating how mixing time, concentration, and diblock copolymer block lengths influence self-assembly in the Flash NanoPrecipitation process.

Simulating Flash NanoPrecipitation at experimental conditions is a challenge for three reasons. First, the final solute and polymer concentrations in Ref. 15 were 1.17 mg/ml, which translates to 30 and 5 solute and copolymer molecules per million solvent molecules, respectively. Second, nanoparticle diameters ranged from 100 to 200 nm.[15] Third, the mixing time was estimated to be a few ms. A simulation at the experimental concentrations capable of forming even a single nanoparticle with a diameter of 100 nm would require $O(10^5)$ solute and polymer molecules, along with $O(10^9)$ solvent molecules, and the time scales are far too long for atomistic simulations. In order to render the problem tractable, a single type of "solvent" particle was employed, with its interactions with the solute and the hydrophobic block of the polymer varying with time. We study mixing times up to 200 μs, an order of magnitude shorter than the estimated mixing times in the experiments. Coarse-graining of the solvent allows us to reduce the number of solvent particles by roughly an order of magnitude. To further reduce the number of solvent molecules, we use solute and polymer concentrations an order of magnitude greater than in the experiments. This only reduces the average distance between solutes and polymers by a factor of $\sim$2.

The structure of this paper is as follows. In Sec. II, we summarize the explicit-solvent model and discuss the simulation methods used in the present work, including the treatment of solvent/anti-solvent mixing. In Sec. III, we present and analyze our simulation results, focusing on the effects of mixing time, solute solubility, solute/polymer concentration, PEG block length, and PS block length. Finally, in Sec. IV, we summarize our results and comment on the remaining challenges associated with modeling Flash NanoPrecipitation.

II. MODEL AND METHODS

Simulations were carried out with the DPD method,[17,18] using the explicit-solvent model of Ref. 16. DPD employs soft, repulsive forces between particles, as well as a random, impulsive force and a frictional, dissipative force, which together act as a thermostat and cause the system to rigorously sample the canonical (NVT) ensemble.[19] We will briefly discuss the parameters used in the model, and we refer the interested reader to Ref. 16 for a complete description of the model parameterization.

The characteristic length, mass, and energy were chosen in Ref. 16 as $L_{\mathrm{DPD}} = 1$ nm, $m_{\mathrm{DPD}} = 200$ Da, and $\varepsilon_{\mathrm{DPD}} = k_B T = 4.114 \times 10^{-21}$ J (at 298 K). This characteristic length permits some coarse-graining of the solute and polymer without erasing structural details entirely. The characteristic mass is equal to the mass of a coarse-grained PS bead, which represents 2 real PS monomers. The intrinsic time scale, derived from non-dimensionalization of the equations of motion, is $\tau_{\mathrm{intrinsic,DPD}} = L_{\mathrm{DPD}}(m_{\mathrm{DPD}}/\varepsilon_{\mathrm{DPD}})^{0.5} = 9$ ps.

As in the previous work, particle masses and cutoff radii for the four types of particles were identical, $m_i = 200$ Da and $r_c = 1$ nm. We used a solvent bead density $\rho = 3.0$ nm^{-3} (reduced density equal to 3). Each solvent monomer represents 11 water molecules, matching the mass density of liquid water. Each solute molecule is represented by a three-bead chain, approximating the solid density of Itraconazole,[15] and the PS portion of the polymer is 5 beads, matching the melt density of polystyrene. The PEG portion of the polymer contains 20 beads, reproducing the radius of gyration for PEG in water.[20] Neighboring beads are held together using harmonic bonds with $r_0 = 0.8$ nm and $k = 0.25$ N/m.

The DPD repulsion parameters and friction coefficients were identical to those of Ref. 16. All like-particle repulsion parameters were set equal to $a_{ii} = 25\varepsilon_{\mathrm{DPD}}$. Solvent-PS and PS-PEG repulsions are $a_{wp} = 54\varepsilon_{\mathrm{DPD}}$ and $a_{pe} = 40\varepsilon_{\mathrm{DPD}}$, matching the critical micelle concentration in water.[21] The solvent-solute repulsion parameter, $a_{ws} = 68\varepsilon_{\mathrm{DPD}}$, was determined from DPD solvent-polymer phase diagrams[22,23] to match the experimental solubility of Itraconazole in water.[15] Two sets of parameters were explored for the solute-PS and solute-PEG repulsion parameters, one representing "favorable" ($a_{sp} = 25\varepsilon_{\mathrm{DPD}}$ and $a_{se} = 35\varepsilon_{\mathrm{DPD}}$) and the other "unfavorable" ($a_{sp} = 35\varepsilon_{\mathrm{DPD}}$ and $a_{se} = 55\varepsilon_{\mathrm{DPD}}$) solute-polymer interactions. Using the relationship developed by Groot and Warren,[17] Flory-Huggins χ-parameters for the interactions between the different types of DPD beads can be calculated. However, caution should be exercised when interpreting these values, since the coarse-grained DPD beads used in our simulations do not represent individual monomers. Maiti and McGrother[24] showed that increasing the degree of coarse-graining leads to an increase in the effective χ-parameter, which explains why the χ-parameters for the interactions in our model are larger than typical experimental values. The friction coefficient was set to $\gamma_{ij} = 500$ ns^{-1} (4.5 in dimensionless units) for all interactions other than the

solvent-solute and solvent-polymer ones. The solvent-solute friction parameter was $\gamma_{ws} = 111$ ns^{-1} (1.0 in dimensionless units) and the solvent-PEG and solvent-PS friction parameters (γ_{we} and γ_{wp}) were 2000 ns^{-1} (18.0 in dimensionless units); this resulted in the correct ratio of the solute diffusion coefficient to the polymer diffusion coefficient.[25]

In Flash NanoPrecipitation, solutes and polymers are initially dissolved in a good solvent (e.g. THF), and then rapidly mixed with water to induce self-assembly. Mixing of solvent and anti-solvent in the laboratory is a complex process that results in spatial inhomogeneities within the mixing chamber.[4,5] To simplify our modeling, we used a single type of solvent particle. In contrast to the previous work that used an instantaneous change in solvent quality, here we vary the solvent-solute and solvent-PS interactions over time as a way of mimicking the decrease in solvent quality. The final repulsion parameters ($a_{wp} = 54\varepsilon_{\mathrm{DPD}}$ and $a_{ws} = 68\varepsilon_{\mathrm{DPD}}$) are pertinent for when the solvent is essentially pure water, after mixing is complete. The initial values of the repulsion parameters are $a_{wp} = 25\varepsilon_{\mathrm{DPD}}$ and $a_{ws} = 25\varepsilon_{\mathrm{DPD}}$, so as to reproduce "good solvent" conditions for the solute and PS block. We ramped these parameters up to $a_{wp} = 54\varepsilon_{\mathrm{DPD}}$ and $a_{ws} = 68\varepsilon_{\mathrm{DPD}}$ over a period of time denoted as the "mixing time," τ_{mix}, in a stepwise fashion over 40 evenly spaced intervals. The solvent-PEG repulsion parameter was kept at a constant value of $a_{we} = 25\varepsilon_{\mathrm{DPD}}$, since both THF and water are good solvents for PEG.

All simulations were carried out using the Highly Optimized Object-oriented Many-particle Dynamics (HOOMD) simulation package.[26,27] A total of 350 simulations required approximately 1000 GPU-days of computing time. A typical simulation run on a single GPU using HOOMD was approximately six times faster than the same simulation run on 16 cores of 2.77-Ghz CPUs using LAMMPS.[28] Each simulation was initialized by randomly placing the solvent beads, solute molecules, and polymers in a square box. The equations of motion for the system were integrated with a time step of $\Delta t = 0.36$ ps at 298 K, and the positions of all solute and polymer particles were output every 1.8 ns for analysis. All of the results presented are the average of 3 to 7 independent simulations carried out under the same conditions but with different initial configurations. Error bars shown in the figures represent 98% confidence intervals of the mean, calculated from duplicate runs.

DPD simulations are known to produce accelerated dynamics (relative to atomistic MD) when the intrinsic time scale is used as a measure of time. As is common in the literature,[29–32] we rescaled time when interpreting simulation results by matching a fundamental dynamic quantity to its experimental value. In this case, we matched the polymer diffusion coefficient to its experimental value by choosing a characteristic time scale $\tau_{\mathrm{DPD}} = 250$ ps, which is roughly 28 times greater than the intrinsic DPD time scale of 9 ps. All results presented in the following sections use this rescaled measure of time.

In order to analyze nanoparticles and micelles during the self-assembly process, we developed an algorithm to identify distinct clusters of solutes and polymers. For the polymers, only the PS portion of the chain was considered during cluster identification. Two molecules were considered to belong to the same cluster if any of the beads in one molecule were within a given cutoff distance of any of the beads in the other molecule. The cluster cutoff distance was taken to be 0.85 nm, roughly the distance at which the first maximum appears in the pair correlation function for a monomeric DPD fluid with $a_{ii} = 25\varepsilon_{\mathrm{DPD}}$ and dimensionless bead density of 3.[22,33] The number of solutes or polymers per nanoparticle (or polymers per micelle) referenced in this study are weight averages. For nanoparticles, only aggregates with at least two solutes (but any number of polymers) are included in the calculation. For micelles, only aggregates containing two or more polymers (but no solute molecules) are included in the calculation.

III. RESULTS AND DISCUSSION

Before presenting our results, we define a "reference system," with respect to which we make perturbations when studying the effects of a given parameter. The reference polymer had a PS block length of 5 and a PEG block length of 20 DPD beads, and the system consisted of 360 150 solvent beads, 450 polymers, and 1200 solute molecules in a 50 nm $\times$ 50 nm $\times$ 50 nm cubic simulation box. The solute and polymer concentrations in the reference system are, respectively, roughly 10 and 20 times higher than in the experimental systems of Kumar *et al.*[15] As stated in the Introduction, we used higher concentrations in order to allow for enough solutes and polymers in the system to form multiple large nanoparticles without having to utilize an impractical system size.

A. Effects of mixing time

In Figure 1, we show the dynamic evolution of the number of solutes and polymers per nanoparticle for systems with favorable solute-polymer interactions. Longer mixing times delay the onset of nanoparticle nucleation, as expected. Although the solvent conditions become poor for the solute before they become poor for the polymer, Figure 1 indicates that for a given system, the number of solutes and polymers per nanoparticle begin to "take off" at the same time. As previously noted, this is because the presence of solute clusters causes polymers to begin aggregating with them, even though the solvent conditions at that point may not yet be poor enough for the polymers to aggregate with one another. Comparing the slopes (in Figure 1) of the number of solutes and polymers per nanoparticle for a given system, one can see that the polymers aggregate in nanoparticles at a slower rate than the solutes. Even when all of the solutes in the system are in stable (no longer growing) nanoparticles, there are still free polymers left in the system. Systems with $\tau_{\mathrm{mix}} = 0$ μs and $\tau_{\mathrm{mix}} = 20$ μs show a more "stepwise" growth pattern of the number of solutes and polymers per nanoparticle.

Systems with unfavorable solute-polymer interactions (not shown) exhibit similar growth patterns, independent of mixing time, concentration, or polymer block lengths. The stepwise pattern is the result of growth through the merging of moderately large nanoparticles, those large enough to

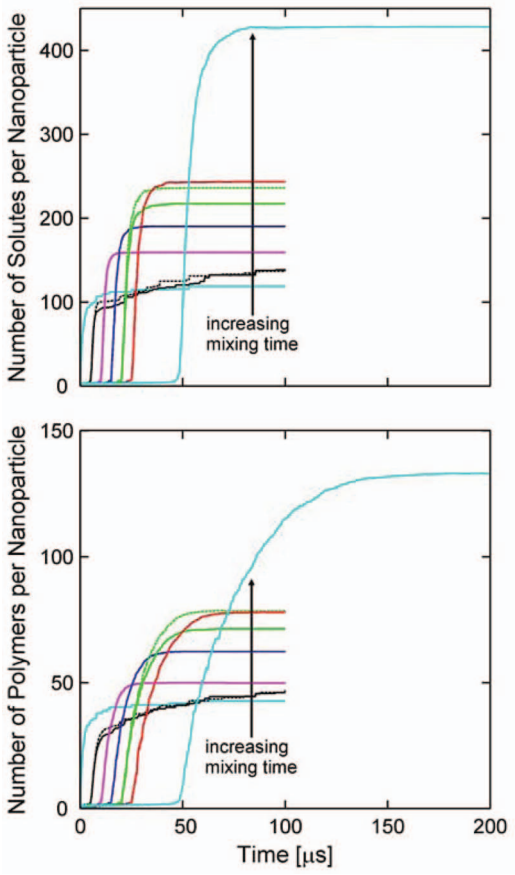

FIG. 1. Number of solutes (top) and polymers (bottom) per nanoparticle versus time for systems with favorable solute-polymer interactions. The mixing times are 0 μs (cyan), 20 μs (black), 40 μs (magenta), 60 μs (blue), 80 μs (green), 100 μs (red), and 200 μs (cyan, top). The dashed lines represent systems with twice as large a simulation volume as their solid-line counterparts.

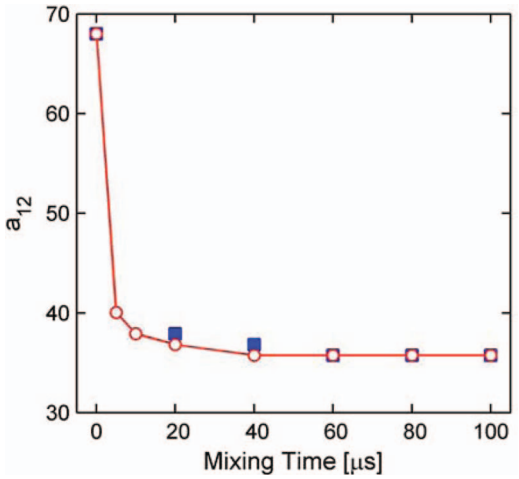

FIG. 2. Value of the solute-solvent interaction parameter, a_{ws}, at the time T_{50} when the weight-averaged number of solutes per nanoparticle reaches 50, for different overall mixing times. The open circles are for systems with unfavorable solute-polymer interactions, and the filled squares are for systems with favorable solute-polymer interactions. The line serves as a guide to the eye. Uncertainties are smaller than symbol sizes.

contribute significantly to the weight-average size at the time of fusion. On the other hand, the smooth growth patterns observed for the systems with favorable solute-polymer interactions and mixing times greater than 40 μs suggest a growth mechanism that involves the fusion of single solutes or small nanoparticles with larger nanoparticles.

We determined the time at which the number of solutes per nanoparticle reached 50, and we then determined the value of the solute-solvent repulsion parameter at that time. Figure 2 indicates that this value of the solute-solvent repulsion parameter is the same for $\tau_{\text{mix}} \geq 40$ μs but is larger for shorter mixing times. Thus, one can categorize the mixing as either "slow" or "fast" with respect to aggregation. For $\tau_{\text{mix}} \leq 20$ μs, the underlying aggregation dynamics are slow relative to mixing, whereas for $\tau_{\text{mix}} \geq 40$ μs, the aggregation dynamics are fast relative to mixing. The difference between these two "mixing regimes" also leads to the aforementioned difference in growth patterns (stepwise versus smooth) seen in Figure 1.

We studied the effects of mixing time on the final nanoparticle size and on the aggregation dynamics of systems with both favorable and unfavorable solute-polymer interactions. Figure 3 shows the final number of solutes and polymers per nanoparticle as a function of mixing time. For two values of the mixing time we performed additional simulations with systems that were twice as large as the reference system, but we found no statistical difference in the results. The number of solute molecules in each nanoparticle increases with mixing time, a result which can be understood by considering the solvent quality as a function of time. Initially, both solute and polymer are soluble. As time progresses, the solvent conditions first start to become poor for the solute, which is present at a higher supersaturation ratio than the polymer; consequently, solute clusters begin to form and collide with one another, resulting in nanoparticle growth. Later, the solvent conditions become sufficiently poor for polymers that the polymers begin to aggregate on the surface of the solute clusters already present. A longer mixing time leads to a longer "window" of time during which the solute has become insoluble but the polymer is still reasonably soluble, giving aggregates more time to collide and fuse before polymers start covering their surfaces and stabilizing them.

Figure 3 also shows that when the solute-polymer interactions are favorable, the number of polymers per nanoparticle increases with mixing time and mirrors the increase in the number of solutes per nanoparticle with mixing time; however, this is not true for the case of unfavorable solute-polymer interactions. The reason is that unfavorable solute-polymer interactions lead to the formation of micelles (polymer aggregates containing no solute molecules), which are not found in the systems with favorable solute-polymer interactions. Figure 4 shows the number of micelles and the number of polymers per micelle formed as a function of mixing time in systems with unfavorable solute-polymer interactions. For all mixing times, the number of polymers per micelle is around ~22, which corresponds to the average aggregation number for this model polymer.[16] The number of micelles increases with mixing time, a result that can also be explained by the changing solubility of the solute and polymer as the solvent

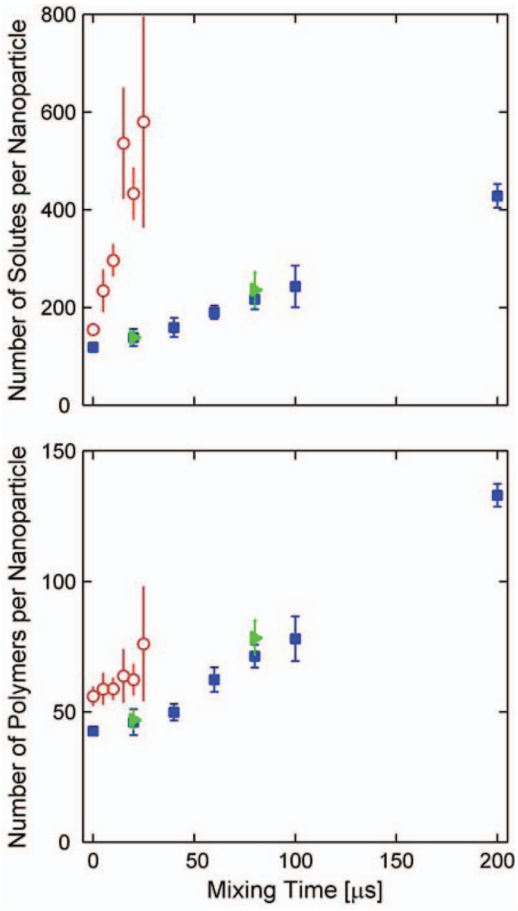

FIG. 3. Final number of solutes (top) and polymers (bottom) per nanoparticle as functions of mixing time. The open circles are for systems with unfavorable solute-polymer interactions, and the filled squares are for systems with favorable solute-polymer interactions. The filled triangles are for the same systems as the corresponding filled squares, but with twice as large a simulation volume.

conditions become poorer during mixing. Based upon the values of the repulsion parameters, the PS blocks in the polymers would prefer to aggregate with one another, rather than sticking to the solute clusters; however, either of these would be preferable to being exposed entirely to the solvent. Longer mixing times lead to a state in which there are fewer, larger solute clusters at the time when the polymers start becoming insoluble. The total surface area of a collection of larger clusters is less than a collection of smaller clusters with the same total volume, and thus, requires fewer polymers to become stabilized. The remaining polymers form micelles, with the number of micelles that form being determined by how much polymer is left after the solute nanoparticles are stabilized.

As observed in Ref. 16, unfavorable solute-polymer interactions lead to clustering of the PS blocks on the nanoparticle surface, leaving regions of the nanoparticle core unprotected by the stabilizing PEG layer. In contrast, favorable solute-polymer interactions lead to a uniform distribution of PS blocks on the core surface and of PEG blocks around the core. As a result, unfavorable solute-polymer interactions lead to the formation of larger nanoparticles, as compared to a system with favorable interactions with the same mixing

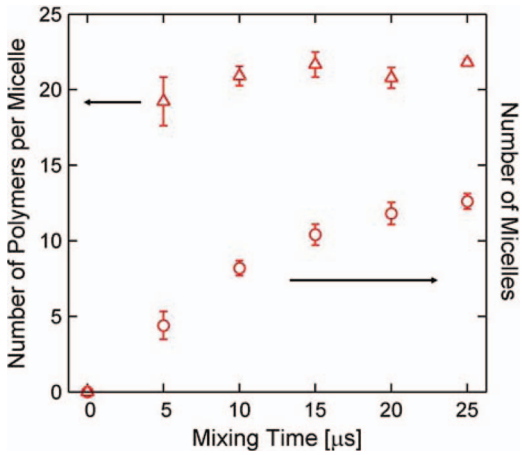

FIG. 4. Number of polymers per micelle (triangles, left axis) and number of micelles (circles, right axis) versus mixing time. Data are shown for systems with unfavorable solute-polymer interactions.

time. Additionally, unfavorable solute-polymer interactions lead to a sharper increase of particle size (primarily given by the number of solutes per nanoparticle) with mixing time, as compared to favorable solute-polymer interactions, since nanoparticles are more likely to fuse with one another upon colliding.

B. Effect of solute solubility

The final value of the solvent-solute repulsion parameter was decreased from $a_{ws} = 68\varepsilon_{\mathrm{DPD}}$ to $a_{ws} = 42\varepsilon_{\mathrm{DPD}}$, a value that is still high enough to render the solute insoluble under the final conditions (one can infer this from the information in Figure 2). We studied this system with both favorable and unfavorable solute-polymer interactions for a mixing time of 20 μs. For the systems with unfavorable solute-polymer interactions, the number of solutes per nanoparticle increases drastically relative to the reference system, with all simulations resulting in the formation of a single large cluster containing all 1200 solute molecules. In this case, the decrease in the solubility of the solute leads to most of the polymers forming stable micelles before the solute molecules begin to aggregate. As a result, very few free polymers are left to stabilize the nanoparticles as they grow. On the contrary, when the solute-polymer interactions are favorable, the number of solutes per nanoparticle decreases relative to the reference system (104 ± 3 for a less soluble solute and 138 ± 19 for the reference system). In this instance, polymer micelles begin to form before solute clusters, but the increased affinity of the solute for the PS block over the solvent causes solutes to become incorporated into the polymer micelles as they are forming. This is a distinctly different mechanism of nanoparticle formation than in the reference system, in which solute clusters form first and are later stabilized by polymers. The strong differences in the way the two systems (favorable and unfavorable solute-polymer interactions) respond to an increase in the solute's solubility provide more evidence[14] that the solute-polymer interactions play a critical role in the outcome of the self-assembly process.

C. Effects of solute and polymer concentration

In order to study the effects of changing the solute and polymer concentrations, we held the number of solutes and polymers fixed (at 1200 and 450, respectively) but increased the system size (and thus, number of solvent particles). We also fixed the number of polymers but varied the number of solutes. The former represents varying the solute and polymer volume fractions while keeping their ratio fixed, while the latter represents varying the solute-polymer ratio at a fixed combined volume fraction. Figure 5 shows the number of solutes per nanoparticle versus overall and relative concentration for systems with unfavorable solute-polymer interactions and $\tau_{\text{mix}} = 5\ \mu$s, and for systems with favorable solute-polymer interactions and $\tau_{\text{mix}} = 40\ \mu$s. At a fixed solute-to-polymer ratio, increasing the overall solute/polymer concentration increases the size of nanoparticles that are formed. During the aggregation process, there are two competing time scales: the time required for a polymer to diffuse to the surface of an aggregate, and the time required for two aggregates to diffuse within a short enough distance to fuse with one another. The diffusion coefficient of the single polymer is significantly higher than that of a large nanoparticle. The characteristic distance separating the polymers and nanoparticles present in the system is longer at lower concentrations. Consequently, more dilute concentrations favor the arrival of a faster-diffusing polymer to the surface of a nanoparticle over another slower-diffusing nanoparticle, since the polymer can visit much more space in the same amount of time. The number of solutes per nanoparticle increases more rapidly with overall concentration for systems with unfavorable solute-polymer interactions than for those with favorable interactions. This is similar to the trend seen in nanoparticle size versus mixing time (Figure 3) and is due to the fact that collisions between nanoparticles with unfavorable solute-polymer interactions are much more likely to result in fusion, due to poorer protection of the nanoparticle core by the surrounding polymer corona.

At a fixed volume fraction of solutes and polymers, increasing the ratio of solute to polymer molecules leads to the formation of larger nanoparticles. This agrees with the experimental results of Gindy *et al*., who also observed an increase in nanoparticle size with an increase in the solute to polymer ratio.[13] As nanoparticles grow, their total surface area decreases and, as seen previously,[16] they become stable when the surface area occupied per polymer becomes small enough that the core is sufficiently shielded by the stabilizing PEG layer. Consider two systems with an equal number of solute molecules, in which one system contains a few large nanoparticles, while the other contains a larger number of small nanoparticles. The system containing the larger nanoparticles requires fewer polymers to stabilize them than the system with the smaller nanoparticles, because the total surface area of the larger nanoparticles is less than that of the smaller ones—this explains the behavior seen in Figure 5. The rate at which the particle size increases with solute-to-polymer ratio is greater for the systems with unfavorable solute-polymer interactions than for those with favorable interactions for the same reason previously mentioned—the poorer protection of nanoparticles during the aggregation process due to PS clustering on the surface when the solute-polymer interactions are unfavorable. We also carried out all of the concentration-effect simulations with instantaneous mixing and found that, qualitatively, the observed trends were identical to the cases of $\tau_{\text{mix}} > 0$ shown in Figure 5.

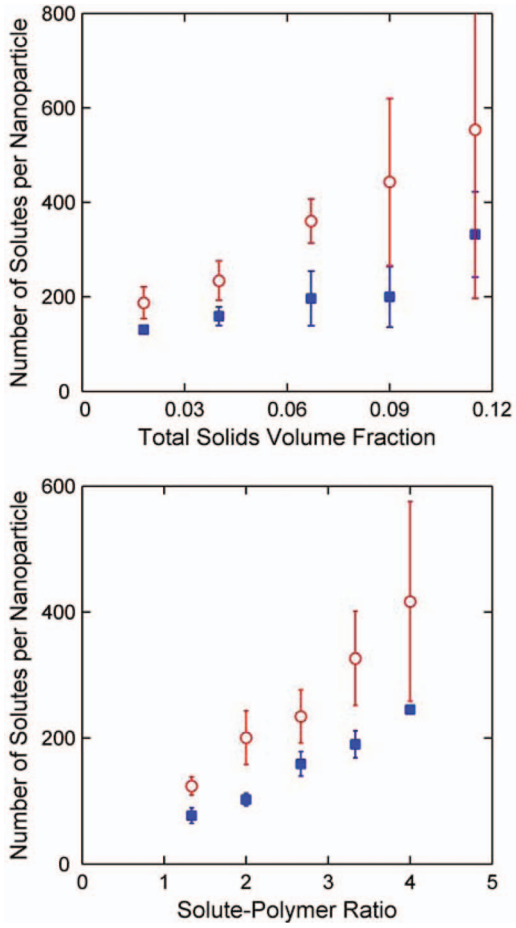

FIG. 5. Number of solutes per nanoparticle for systems with different total solids volume fractions, but a fixed solute-polymer ratio (top), and systems with different solute-polymer ratios, but a fixed total solids volume fraction (bottom). The open circles are for systems with unfavorable solute-polymer interactions and $\tau_{\text{mix}} = 5\ \mu$s, and the filled squares are for systems with favorable solute-polymer interactions and $\tau_{\text{mix}} = 40\ \mu$s.

D. Effects of PEG and PS block lengths

In order to study the effect of changing the length of the PEG block of the polymer, we ran simulations of the reference system and varied only the number of coarse-grained PEG beads in each polymer, keeping the *number* of polymers constant. Figure 6 shows the number of solutes per nanoparticle versus PEG block length for both instantaneous and non-instantaneous mixing. In both cases, we find that nanoparticle size decreases with an increase in PEG block length. An increase in the PEG block length (while fixing the number of solutes, number of polymers, and the system size) affects the polymer's critical micelle concentration, its diffusion coefficient, and the surface area that it is capable of covering on a nanoparticle's surface. All three of these effects can

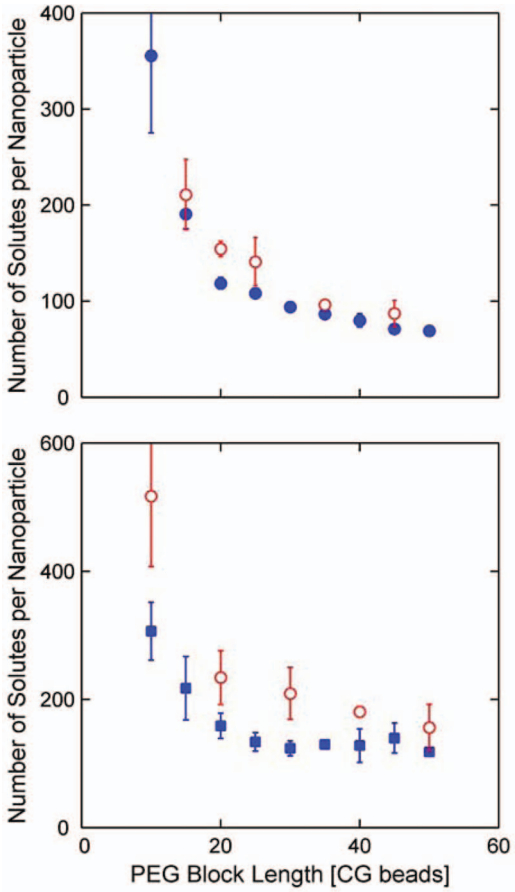

FIG. 6. Number of solutes per nanoparticle versus PEG block length for systems with instantaneous (top) and finite (bottom) mixing times. The open circles are for systems with unfavorable solute-polymer interactions, and the filled squares are for systems with favorable solute-polymer interactions.

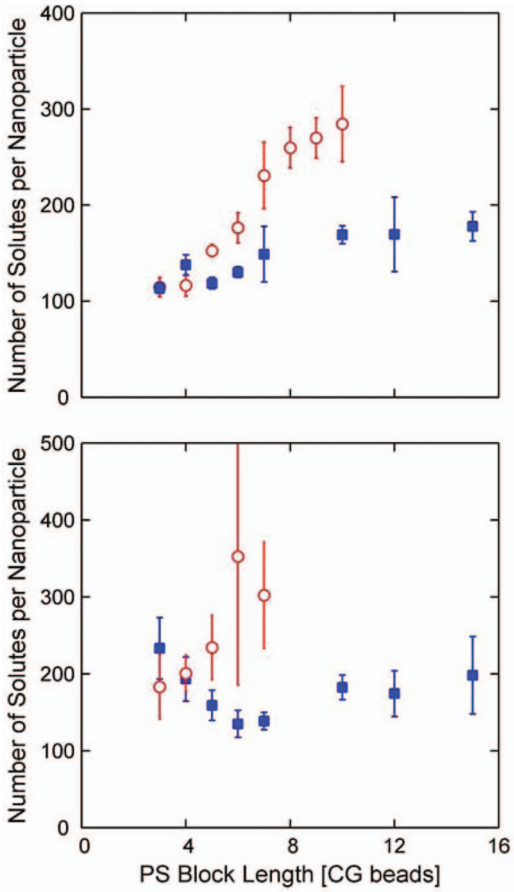

FIG. 7. Number of solutes per nanoparticle versus PS block length for systems with instantaneous (top) and finite (bottom) mixing times. Symbols are as in Figure 6.

influence final nanoparticle size. Increasing the length of the PEG block of the copolymer (while fixing the PS block length) increases its critical micelle concentration.[16,34,35] Based solely on this fact, an increase in PEG length should lead to larger particles, since longer PEG blocks lead to higher polymer solubility at any point during the mixing process. Additionally, a longer PEG block decreases the diffusion coefficient of the polymer—based solely on this fact, the particle size should also decrease with an increase in PEG block length, since the polymers should take longer to find a nanoparticle's surface. Finally, increasing the PEG block length permits each polymer to sterically screen a larger area of the nanoparticle surface—based solely on this reasoning, a longer PEG block should lead to smaller nanoparticles, since they would then require fewer polymers on their surfaces to be sufficiently protected. In our system, in the range of parameter space explored, the third effect wins out over the other two—that is, even though the longer PEG blocks lead to more soluble polymers and lower polymer diffusion coefficients (both of which should make the nanoparticle size larger), the dominant effect is that longer PEG blocks can protect a larger area of the nanoparticle core.

We also studied the effect of the PS block length by running simulations of the reference system and varying only the number of coarse-grained PS beads in each polymer, keeping the number of polymers in the system constant. Figure 7 shows the final number of solutes per nanoparticle versus PS block length for systems with instantaneous mixing and for systems with a finite mixing time ($\tau_{\text{mix}} = 40\ \mu$s for systems with favorable solute-polymer interactions and $\tau_{\text{mix}} = 5\ \mu$s for those with unfavorable interactions). For instantaneous mixing, we observe an increase in nanoparticle size with PS block length for both favorable and unfavorable solute-polymer interactions, with this trend being more pronounced when the interactions are unfavorable.

For systems with unfavorable solute-polymer interactions and $\tau_{\text{mix}} = 5\ \mu$s, we also find that the particle size increases with PS block length. Figure 8 shows a few snapshots taken from a simulation with a PS block length of 7. In the first snapshot, a number of large nanoparticles are present, but some of the polymers and solutes still remain in the system as free monomers. In the second snapshot, the solvent quality has become poor enough that all of the polymers have either stuck to the surfaces of nanoparticle clusters or aggregated with one another to form micelles. By the third snapshot, some of the nanoparticles have fused with one another or absorbed micelles. Finally, in the last snapshot, which is $\sim$80 μs after the third snapshot, some of the nanoparticles have aggregated further, while the number of micelles in the simulation remains unchanged. A movie of the simulation represented in

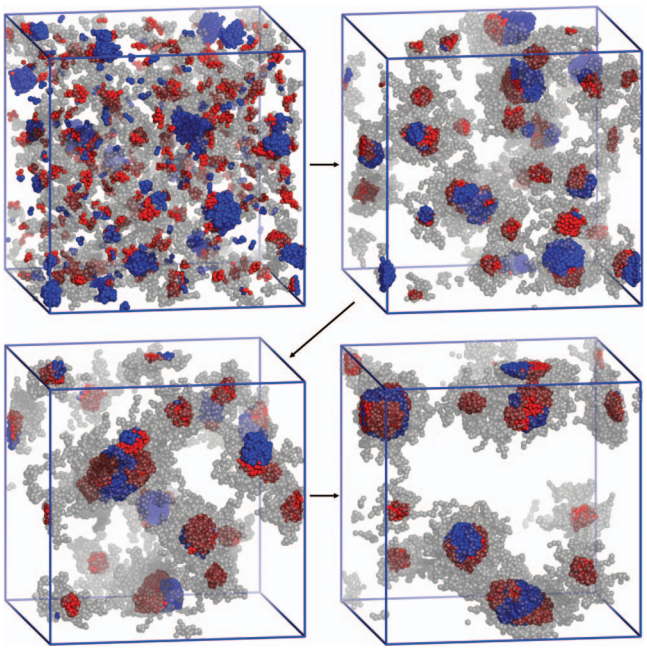

FIG. 8. Snapshots from a system with unfavorable solute-polymer interactions and $\tau_{mix} = 5$ μs, in which the PS block has a length of 7. The snapshots shown were taken at 2 μs, 6 μs, 12.5 μs, and 100 μs, with the arrows showing the appropriate order. The solute beads are shown in blue, the PS beads in red, and the PEG beads in transparent grey (enhanced online). [URL: http://dx.doi.org/10.1063/1.3653379.1]

Figure 8 is available (see Figure 8). It is also worth noting that for systems with unfavorable solute-polymer interactions and a PS block length of 3, micelles form at intermediate times but break up at later times, with no free polymers or micelles remaining at the end of the simulations.

Finally, we find that for systems with favorable solute-polymer interactions and a mixing time of 40 μs, the particle size as a function of PS block length exhibits a well-defined local minimum, as seen in Figure 7. Figure 9 shows the dynamic evolution of particle size and reveals that the growth mechanism changes when the PS block length reaches ~6. For shorter PS block lengths, the particles grow via the "smooth" dynamics described earlier, in which the dominant growth mechanism is the fusion of single solute molecules or small nanoparticles with larger nanoparticles. However, for longer PS block lengths, a "stepwise" growth pattern is observed, which is indicative of the fusion of larger nanoparticles with one another.

In order to visually differentiate these two mechanisms, we show snapshots of simulations with favorable solute-polymer interactions and a PS block length of 3 (Figure 10) and 12 (Figure 11). From the second snapshot in Figure 10, one can see that when all of the solute molecules have aggregated into nanoparticles, many of the polymers still exist as free monomers. By the third snapshot, many of the polymers have been absorbed onto the surfaces of the nanoparticles; finally, in the last snapshot, all of the polymers are on nanoparticle surfaces. Between the second and fourth frames, however, none of the nanoparticles fused with one another. Evidently, there is a sufficient number of polymers on the nanoparticles by the time of the second

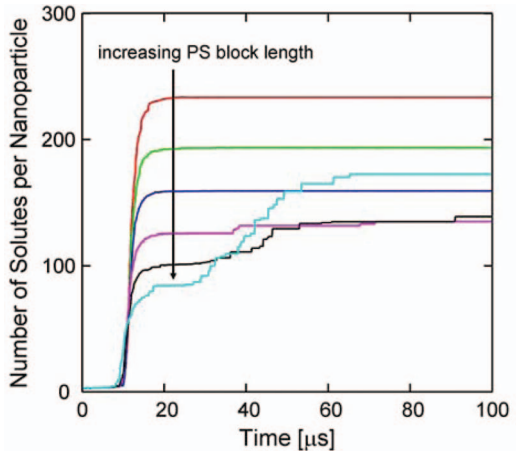

FIG. 9. Number of solutes per nanoparticle versus time for systems with favorable solute-polymer interactions and $\tau_{mix} = 40$ μs, but with different PS block lengths. The PS block lengths are 10 (cyan), 7 (black), 6 (magenta), 5 (blue), 4 (green), and 3 (red).

snapshot to stabilize them. In contrast, the first snapshot of Figure 11 shows that when all of the polymers (with a PS block length of 12) in the system are found in nanoparticles, free solutes still remain. Between the second and fourth snapshots the number of nanoparticles decreases, indicating that fusion of nanoparticles has occurred. Although the nanoparticles in the second snapshot contain a significant number of PS beads at the surfaces of their cores, evidently, the stabilizing PEG layers around the cores are not dense enough to fully prevent the nanoparticles from fusing. Movies of the simulations represented in Figures 10 and 11 are available (see Figures 10 and 11).

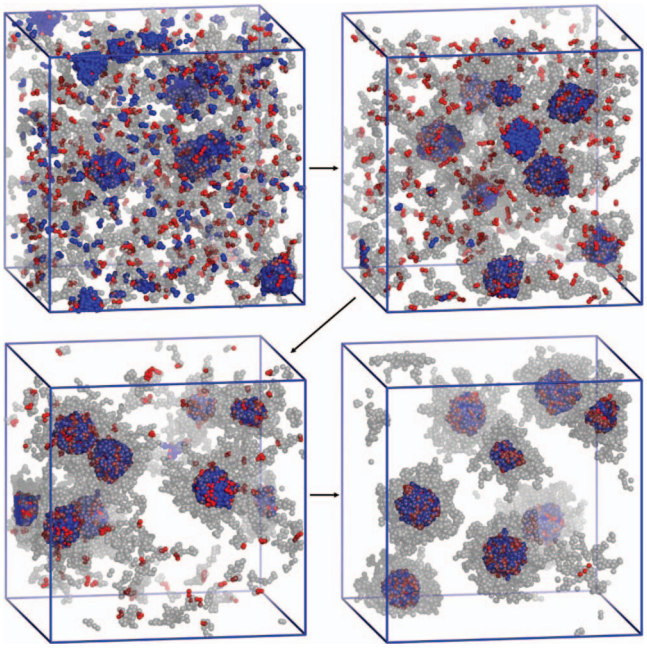

FIG. 10. Snapshots from a system with favorable solute-polymer interactions and $\tau_{mix} = 40$ μs, in which the PS block has a length of 3. The snapshots shown were taken at 12.5 μs, 17.5 μs, 25 μs, and 100 μs, with the arrows showing the appropriate order. Beads are colored as in Figure 8 (enhanced online). [URL: http://dx.doi.org/10.1063/1.3653379.2]

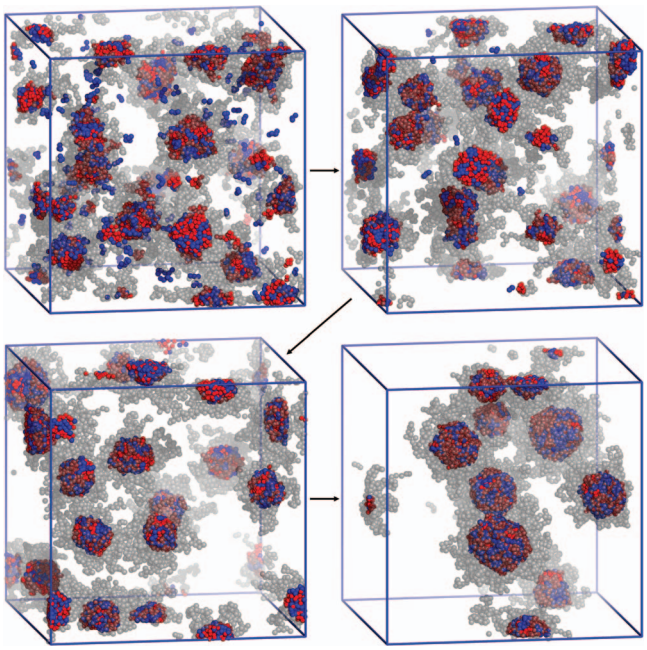

FIG. 11. Snapshots from a system with favorable solute-polymer interactions and $\tau_{mix} = 40\ \mu s$, in which the PS block has a length of 12. The snapshots shown were taken at 11.5 μs, 16 μs, 28 μs, and 100 μs, with the arrows showing the appropriate order. Beads are colored as in Figure 8 (enhanced online). [URL: http://dx.doi.org/10.1063/1.3653379.3]

IV. CONCLUSIONS

We have used a previously developed explicit-solvent DPD model[16] to simulate the Flash NanoPrecipitation process, focusing on the effects of mixing time, solute solubility, solvent and polymer concentrations, and polymer block lengths on the aggregation dynamics and final particle size. The model was parameterized by matching key experimental properties of the solute, polymer, and solvent used in the experiments of Kumar *et al.*[15] We found that nanoparticle size increases with mixing time, due to the differing solubilities of the solute and polymer. At the concentration studied, we found that for $\tau_{mix} \geq 40\ \mu s$, the aggregation dynamics are fast relative to mixing, whereas for $\tau_{mix} \leq 20\ \mu s$, the aggregation dynamics are slow relative to mixing. An increase in the solubility of the solute was found to produce larger nanoparticles when the solute-polymer interactions were unfavorable and smaller nanoparticles when the interactions were favorable. Sufficiently increasing the solute's solubility causes polymers to begin aggregating with one another before solutes aggregate with one another, and the solute-polymer interaction dictates whether or not the free solutes have an affinity for the PS core of the micelles.

We also showed that either an increase in the overall concentration of solutes and polymers (while keeping their ratio fixed) or an increase in the ratio of solutes to polymers (at fixed total concentration) leads to larger nanoparticles (for both instantaneous and non-instantaneous mixing). Additionally, we found that an increase in PEG block length produced smaller nanoparticles, the dominating effect being the increase in nanoparticle surface area covered by each polymer. These trends were more pronounced when the solute-polymer interactions were unfavorable. This is a result of an increased likelihood of nanoparticles fusing upon collision when the solute-polymer interactions are unfavorable, due to non-uniform surface coverage by the polymer. Finally, a non-monotonic change in particle size with hydrophobic block length was observed for systems with favorable solute-polymer interactions and slow mixing (relative to self-assembly). This result indicates that there may be experimentally "optimal" copolymer architectures for researchers looking to limit particle size.

While the specific details of our results (e.g. final particle size) depend on the model parameters, even with relatively large changes in them, the final structures observed are still polymer-protected nanoparticles. An additional indication of the relatively limited sensitivity of the qualitative aspects of the aggregation physics on model parameters is provided in Ref. 16, in which substantially different potentials and coarse-grained mappings were employed between the different components, but the final structure of the nanoparticles was found to be very similar to those formed with the DPD model employed in the present work.

Although our results can serve as a guide to experimentalists in their efforts, we are still far from simulating systems at experimental conditions. Even with a coarse-grained model, we were forced to investigate solute and polymer concentrations roughly an order of magnitude greater than those seen in experiments. Furthermore, the mixing times we investigated were also an order of magnitude less than those used in experiments. Even with these simplifications, our simulations required a massive investment in computing time (1000 GPU-hours). Despite the increase in computational efficiency from the use of GPUs, a direct simulation of a system with experimental concentrations, mixing times, and nanoparticles sizes is still elusive.

ACKNOWLEDGMENTS

Financial support for this work was provided by a NIRT award from the National Science Foundation (CBET-0506966), with additional support from the Princeton Center for Complex Materials, a NSF MRSEC (Award DMR-0819860), from NSF grant CMMI-1002469, and from DOE grant DE-SC0002097. The authors are grateful for discussions with Professor Robert K. Prud'homme, Dr. Varun Kumar, and Suzanne M. D'Addio.

[1]B. K. Johnson and R. K. Prud'homme, Aust. J. Chem. **56**, 1021 (2003).
[2]B. K. Johnson and R. K. Prud'homme, Phys. Rev. Lett. **91**, 118302 (2003).
[3]B. K. Johnson and R. K. Prud'homme, AIChE J. **49**, 2264 (2003).
[4]Y. Liu, C. Y. Cheng, R. K. Prud'homme, and R. O. Fox, Chem. Eng. Sci. **63**, 2829 (2008).
[5]J. C. Cheng and R. O. Fox, Ind. Eng. Chem. Res. **49**, 10651 (2010).
[6]B. Ungun, R. K. Prud'homme, S. J. Budijono, J. N. Shan, S. F. Lim, Y. G. Ju, and R. Austin, Opt. Express **17**, 80 (2009).
[7]V. Kumar, D. H. Adamson, and R. K. Prud'homme, Small **6**, 2907 (2010).
[8]S. J. Budijono, J. N. Shan, N. Yao, Y. Miura, T. Hoye, R. H. Austin, Y. G. Ju, and R. K. Prud'homme, Chem. Mat. **22**, 311 (2010).
[9]M. E. Gindy and R. K. Prud'homme, Expert Opin. Drug Deliv. **6**, 865 (2009).
[10]S. M. D'Addio, C. Kafka, M. Akbulut, P. Beattie, W. Saad, M. Herrera, M. T. Kennedy, and R. K. Prud'homme, Mol. Pharm. **7**, 557 (2010).

[11]V. Kumar, S. Y. Hong, A. E. Maciag, J. E. Saavedra, D. H. Adamson, R. K. Prud'homme, L. K. Keefer, and H. Chakrapani, Mol. Pharm. **7**, 291 (2010).
[12]M. Akbulut, P. Ginart, M. E. Gindy, C. Theriault, K. H. Chin, W. Soboyejo, and R. K. Prud'homme, Adv. Funct. Mater. **19**, 718 (2009).
[13]M. E. Gindy, A. Z. Panagiotopoulos, and R. K. Prud'homme, Langmuir **24**, 83 (2008).
[14]T. Chen, S. M. D'Addio, M. T. Kennedy, A. Swietlow, I. G. Kevrekidis, A. Z. Panagiotopoulos, and R. K. Prud'homme, Nano Lett. **9**, 2218 (2009).
[15]V. Kumar, L. Wang, M. Riebe, H. H. Tung, and R. K. Prud'homme, Mol. Pharm. **6**, 1118 (2009).
[16]J. R. Spaeth, I. G. Kevrekidis, and A. Z. Panagiotopoulos, J. Chem. Phys. **134**, 164902 (2011).
[17]R. D. Groot and P. B. Warren, J. Chem. Phys. **107**, 4423 (1997).
[18]P. J. Hoogerbrugge and J. Koelman, Europhys. Lett. **19**, 155 (1992).
[19]P. Espanol and P. Warren, Europhys. Lett. **30**, 191 (1995).
[20]S. Kawaguchi, G. Imai, J. Suzuki, A. Miyahara, and T. Kitano, Polymer **38**, 2885 (1997).
[21]K. Mortensen, W. Brown, K. Almdal, E. Alami, and A. Jada, Langmuir **13**, 3635 (1997).
[22]J. R. Spaeth, T. Dale, I. G. Kevrekidis, and A. Z. Panagiotopoulos, Ind. Eng. Chem. Res. **50**, 69 (2010).
[23]C. M. Wijmans, B. Smit, and R. D. Groot, J. Chem. Phys. **114**, 7644 (2001).
[24]A. Maiti and S. McGrother, J. Chem. Phys. **120**, 1594 (2004).
[25]L. M. Bronstein, D. M. Chernyshov, G. I. Timofeeva, L. V. Dubrovina, P. M. Valetsky, and A. R. Khokhlov, Langmuir **15**, 6195 (1999).
[26]C. L. Phillips, J. A. Anderson, and S. C. Glotzer, J. Comput. Phys. **230**, 7191 (2011).
[27]J. A. Anderson, C. D. Lorenz, and A. Travesset, J. Comput. Phys. **227**, 5342 (2008).
[28]S. Plimpton, J. Comput. Phys. **117**, 1 (1995).
[29]R. D. Groot, Langmuir **16**, 7493 (2000).
[30]R. D. Groot and K. L. Rabone, Biophys. J. **81**, 725 (2001).
[31]R. D. Groot, J. Chem. Phys. **118**, 11265 (2003).
[32]R. M. Fuchslin, H. Fellermann, A. Eriksson, and H.-J. Ziock, J. Chem. Phys. **130**, 214102 (2009).
[33]I. V. Pivkin and G. E. Karniadakis, J. Chem. Phys. **124**, 184101 (2006).
[34]M. A. Floriano, E. Caponetti, and A. Z. Panagiotopoulos, Langmuir **15**, 3143 (1999).
[35]K. Meguro, Y. Takasawa, N. Kawahashi, Y. Tabata, and M. Ueno, J. Colloid Interface Sci. **83**, 50 (1981).